

CHAPTER 6

Raman Optical Activity (ROA) Studies on Chiral Materials: BINAP

(2,2'-bis (diphenylphosphino)-1,1'-binaphthyl) (C₄₄H₃₂P₂)

Abstract

Mother Nature is home to several chiral molecules that exist in two stereoisomeric forms that are non-superimposable mirror images of each other. Chiral molecules are used as an active pharmaceutical ingredient (active pharmaceutical agent-API) to prepare chiral drugs (pharmacology), present in flavours, herbicides, and insecticides. It is essential to understand the differences between two enantiomers of chiral molecules since they have different biological activities. In the present work, we have investigated non-hydrostatic high-pressure effects on the chiral molecule 2,2'-bis (diphenyl phosphino)-1,1' binaphthyl (BINAP) (C₄₄H₃₂P₂) with the help of *in-situ* Raman optical activity (ROA).

BINAP is an axial chiral molecule that is commonly used in asymmetric synthesis and exists in two stereoisomeric forms. (Yu et al., 2000) Both of the enantiomers have similar chemical and physical properties but differ in their optical activity (the ability to rotate plane-polarized light in the opposite direction). Its two stereoisomeric forms are R BINAP and S BINAP and both crystallize in monoclinic form with space group P2₁ and C₂ symmetry. (Wu et al., 2020) Using Syntek symmetric diamond anvil cell (DAC), R BINAP was compressed up to 11.77 GPa and S BINAP 12.62 GPa respectively, in a non-hydrostatic pressure environment. Raman and Raman optical activity (ROA) spectra were recorded to understand the effects. Since BINOL has a comparable structure and axial chirality to that of BINAP, the mode assignments were made with respect to BINOL.

Raman spectra at ambient conditions for both enantiomers were found to be the same and overlap with each other, while Raman Optical Activity (ROA) spectra of both enantiomers at the ambient environment were opposite of each other. With compression, the Raman spectra for both enantiomers (R BINAP and S BINAP) show similar changes at the same pressure. At a very low pressure of 0.4 GPa, both enantiomers exhibit a change in $d\omega/dP$ and a further change was observed at a pressure around 2 GPa. Peaks $\sim 1031\text{ cm}^{-1}$ ($\nu_{C_6-C_7}$, $\delta_{C_6-C_7-C_8}$, $\delta_{C_5-C_6-C_7}$, δ_{C_5-H} , δ_{C_6-H} , δ_{C_7-H} , δ_{C_8-H}) $\sim 1378\text{ cm}^{-1}$ ($-\nu_{C_9-C_{10}}$, δ_{O-H} , ν_{C_2-O}), and $\sim 1591\text{ cm}^{-1}$

$^1(\nu_{C_1-C_1'}, \nu_{C_2-C_3}, \nu_{C_6-C_7}, \nu_{C_9-C_{10}}, \delta_{O-H})$ show splitting around 2 GPa. The effects on both enantiomers were partially reversible after decompression, showing that pressure has an irreversible impact on the chirality of both enantiomers.

However, the ROA spectra in the ambient environment for both enantiomers were found to be opposite of each other. It was observed that the chirality of both enantiomers was switched at a modest pressure of 0.08 GPa. ROA was still observed above 0.08 GPa for a few peaks, but once switched, chirality was not reversed. On decompression for R BINAP, no ROA was switched back, but for S BINAP, ($\sim 1003 \text{ cm}^{-1}$, $\sim 1378 \text{ cm}^{-1}$ ($-\nu_{C_9-C_{10}}$, δ_{O-H} , ν_{C_2-O}), show some reversibility, but only with respect to peak positions and not with respect to peak intensity. On decompression, ROA spectra show partial reversibility, revealing that the chirality of both enantiomers is affected by pressure.

Raman and Raman Optical Activity (ROA) studies of both enantiomers in non-hydrostatic pressure environment provide insight into irreversible chirality switching in an axially chiral molecule, BINAP. Our results are first of their kind to give information about the switching chirality in an axially chiral molecule, at very low pressures comparable to those used in tableting. These findings will be immensely helpful to the pharmaceutical industry since enantiomer can switch its chirality during the pelletization process and can change the functionality of a drug molecule, turning it out to be hazardous.

6.1 Introduction

Chiral molecules are of biological and pharmaceutical interest. As they are used as active pharmaceutical ingredients (API) to make drugs. (Abram et al., 2019; Blaser, 2013; Brooks et al., 2011; Ceramella et al., 2022; Nguyen et al., 2006; Sanganyado et al., 2017; Zhou et al., 2018) Chiral molecules exist in two stereoisomeric forms with the same formula and the same physical and chemical properties. The differences in their biological activities make it essential to know the optical activity of both enantiomers, as each enantiomer have their own pharmacological activity. It is possible that one enantiomer can cure, but the other enantiomer can be hazardous or completely inactive. Knowledge of the correct enantiomer will lead to the formation of the right drug. (Eriksson et al., 2001; Kim & Scialli, 2011; Newbronner & Karl Atkin, 2017; Woolf, 2022)

Optical rotatory dispersion (ORD) and circular dichroism (CD) are sensitive spectroscopic techniques to analyze chirality in molecules. (D. D. G. Snatzke, 1968; W. Woody, 1995) In

optical rotatory dispersion (ORD), variation in optical rotation is measured with respect to the change in wavelength (differential refraction),(Castiglioni et al., 2011; Eyring et al., 1968) while in circular dichroism (CD), the differential absorption of left and right circularly polarized light is analyzed (Eyring et al., 1968; G. Snatzke, 1968; W.Woody, 1995). Both ORD and CD techniques are related to electronic transitions and measure electronic optical activity. The vibrational spectrum is useful for extracting more detailed stereochemical information from an optically active chiral molecule because it contains more structure-sensitive bands than the electronic spectrum and can provide more conformational details of the chiral molecules. (Laurence D Barron et al., 2007)

Vibrational Optical activity (VOA) is a powerful spectroscopic technique that is a combination of vibrational spectroscopy and optical activity. (Polavarapu. Prasad L, 2002) It provides more detailed stereochemical information of chiral molecules as it analyzes the optical activity of (chiral) molecules with their vibrational spectrum. Due to its sensitivity to molecular structure, this technique is now widely accepted. (Fujisawa & Unno, 2020)

In Vibrational Optical Activity (VOA), left and right circularly polarized light are analyzed with molecules that undergo vibrational transitions. It has two branches: Vibrational Circular Dichroism (VCD) and Vibrational Raman Optical Activity (ROA). Both vibrational optical activity techniques provide a plethora of stereochemical and conformational details of chiral molecule. (Spencer et al., 1988) In VCD differential absorption of left and right infrared circularly polarized light is analyzed (vibrational transitions) that occur in the infrared region of spectrum. (A.Nafie, 1999; Laurence D Barron et al., 2007) Raman Optical activity is another chirality sensitive spectroscopic technique and was discovered by Atkins and Barron in 1969. They depicted when light is scattered from chiral molecule (optically active molecule), scattered intensity depends upon incident light's circular polarization. (Atkins & Barron, 1969)(Atkins and Barron in 1969) They observed small difference in the vibrational Raman scattering intensities when right and left circularly polarized light was incident on chiral molecule.(L D Barron et al., 2002; Laurence D. Barron, 2015)

In recent years ROA an analogue of VCD has emerged as a powerful spectroscopic technique. ROA instrumentation varies for measuring vibrational optical activity as it depends on whether polarization modulation is performed on an incident or scattered path. (Hecht & Barron, 1994) Due to different polarization states, four different types of ROA setups exist: Incident Circular Polarization (ICP) ROA, Scattered Circular Polarization (SCP) ROA, Dual Circular

Polarization I (DCP_I) ROA, and Dual Circular Polarization II (DCP_{II}) ROA. In (ICP) ROA small difference in the intensity of Raman scattering from chiral molecules is measured when left and right circularly polarized light are incident on the sample. Schematic of ICP (ROA) is shown in Figure 6.1a. In (SCP) ROA, the small circularly polarized component present in the scattered light is measured when light of fixed polarization is allowed to fall on the sample as shown in Figure 6.1b. (Laurence D. Barron, 2015). In dual circular polarization two forms exist: when incident and scattered circular polarizations are in phase, it is (DCP_I) ROA, as in Figure 6.1c and when incident and scattered circular polarizations are out of phase, it is (DCP_{II}) ROA shown in Figure 6.1d. (Nafie et al., 1991)

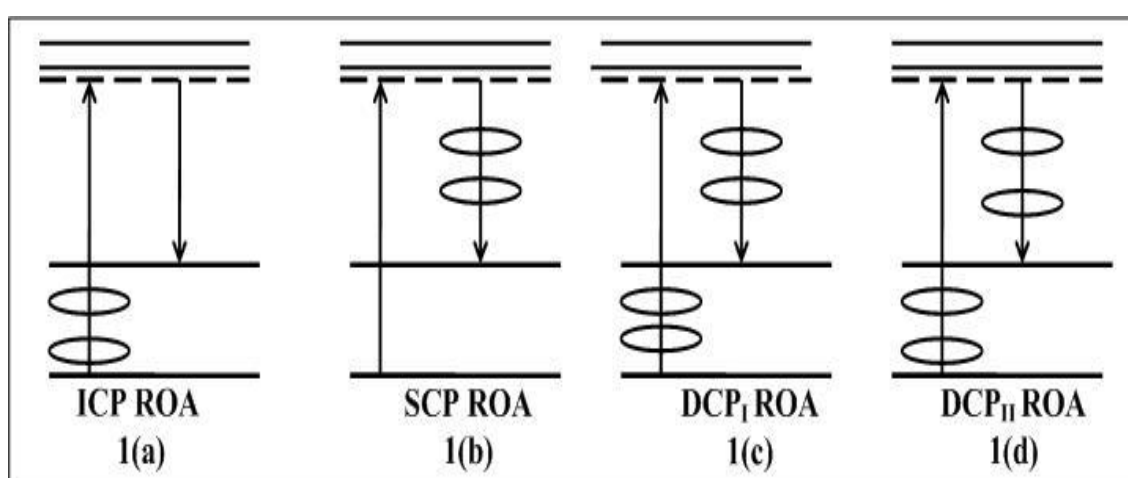


Figure 6.1: Different types of Raman Optical Activity. (Nafie et al., 1991)

Recently an extension of ROA is measured, by combining ROA with Surface enhanced Raman spectroscopy (SERS). Surface enhanced Raman Optical activity (SEROA) studies the vibrational transitions of optically active chiral molecules in left and right circularly polarized light. (Abdali & Blanch, 2008; Das et al., 2021)

Raman Optical Activity (ROA) is sensitive to optically active chiral molecules and varies due to the vibrational coordinates of optically active molecule. (Laurence D. Barron & Buckingham, 1971) Raman scattering mechanism is due to the interference between the light waves scattered due to the molecular polarizability and optical activity tensors of the chiral molecule. Scattered intensity completely depends upon the degree of incident circular polarization and the component of circular polarization that are present in the scattered light. (Laurence D. Barron, 2015)

Later, in 1971, Barron and Buckingham proposed a dimensionless parameter known as "circular intensity difference" (CID), which is represented by Δ . When right and left circularly

polarized light is incident on an optically active molecule, there is a minute difference in Raman scattering intensities, and this difference is denoted by Eq. 1.

$$\Delta = \frac{I^R - I^L}{I^R + I^L} \quad (1)$$

Where I^R and I^L are scattered intensities when right and left circularly polarized light is incident on optically active molecule. (Laurence D. Barron & Buckingham, 1971)

Barron et.al in 1973 observed Raman Optical Activity in an optically active chiral molecule in its liquid phase for the first time and introduced polarizability tensors. (L. D. Barron et al., 1973; Laurence D. Barron, 2015; Laurence D Barron et al., 2007) Electric dipole-electric dipole molecular polarizability tensor $\alpha_{\alpha\beta}$, electric dipole- magnetic dipole optical activity tensor $G'_{\alpha\beta}$, and electric dipole- electric quadrupole optical activity tensor $A_{\alpha\beta\gamma}$. (Laurence D. Barron, 2015).

ROA scattering data can be collected in different geometries: forward (0°), right-angle (90°), and backward path (180°) "Circular intensity difference" (CID) expressions for forward (0°) and backward scattering geometries (180°) are given by Eq. 2 and Eq. 3.(Laurence D. Barron, 2015; Laurence D Barron et al., 2007)

$$\Delta(0^\circ) = \frac{4[45\alpha G' + \beta(G')^2 - \beta(A)^2]}{c[45\alpha^2 + 7\beta(\alpha)^2]} \quad (2)$$

$$\Delta(180^\circ) = \frac{24[\beta(G')^2 + \frac{1}{3}\beta(A)^2]}{c[45\alpha^2 + 7\beta(\alpha)^2]} \quad (3)$$

Conventional Raman scattering intensities are the same in backward and forward directions while backscattering enhances the intensity of ROA. ROA in the solid state is now encouraged, as when solid samples are exposed to circularly polarized light, it disturbs their polarization.(Duan et al., 2015; Shimoaka et al., 2019) Several modes of Raman spectra match with Raman Optical activity modes.(Shimoaka et al., 2019)

6.2 Materials and Methods

In-situ high pressure Raman spectroscopic and Raman Optical Activity (HP-ROA) experiments were performed on both enantiomers of 2, 2'- bis (diphenyl phosphino)- 1,1' binaphthyl. 2, 2'- bis (diphenyl phosphino) - 1,1' binaphthyl is an organophosphorus compound and well known as BINAP. (Berthod et al., 2005; Noyori & Takaya, 1990) It is widely used in asymmetric synthesis and consists of 2-diphenyl phosphino naphthyl groups linked at 1-1' positions with the single bond as shown in Figure 6.2. Rotation about the single bond is restricted due to the steric hindrance of the phosphine groups (atropisomerism). BINAP lacks chiral center due to C_2 symmetric framework and possess axial chirality. The dihedral angle between the naphthyl groups is approximately 90° . It exists in two stereoisomeric forms R BINAP and S BINAP, both are non-superimposable mirror images of each other and both are used in asymmetric synthesis. (Noyori & Takaya, 1990)

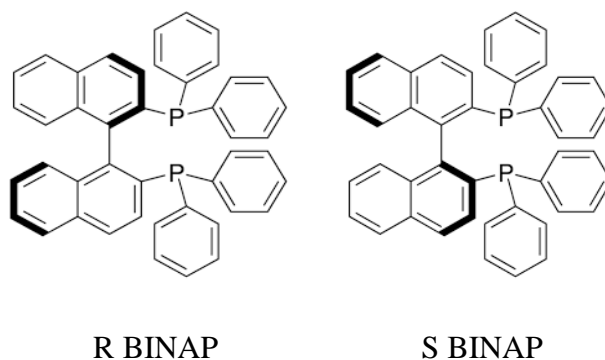


Figure 6.2: Chemical structure of R BINAP and S BINAP.

R BINAP CAS-76189-55-4 [α]_{20/D} +222° and S BINAP CAS-76189-56-5 [α]_{20/D} -222° were purchased from Sigma-Aldrich and were used for the experiment without any additional purification. The samples were stored in a tightly packed vial with proper nitrogen purging and were kept in a vacuum desiccator.

High pressure experiments were performed on a Syntek symmetric DAC diamond anvil cell with Type I diamonds, with a culet size of 400 microns. The sample for the experiment was contained in a stainless-steel gasket (T301) of preindented thickness of 50 microns with a centrally drilled hole of size ~ 130 microns. In order to generate a non-hydrostatic pressure environment, the sample was filled within the sample cavity with no surrounding media.

A single-frequency Oxxius laser operating at 532 nm was used as an excitation source. A spectrometer model SR-500i-A-R with 1800 lines/mm grating was used to record the Raman spectra attached to the thermoelectrically cooled Andor iDUS charge coupled device camera.

For High Pressure Raman Optical Activity (HP-ROA) Spectroscopic experiments, circularly polarized light was generated using zero order quarter wave plate fabricated for 532nm (Holmarc). A single-frequency Oxxius laser operating at 532 nm generated plane polarized laser light vibrating in perpendicular plane. It is allowed to fall on the quarter wave plate oriented at $+45^\circ$ and -45° with respect to polarization direction of laser beam, to generate right and left circularly polarized light. (Gribble & Hall, 1993; Nesse, 1991) In backscattering path Lyot depolarizer (Holmarc) made up of quartz crystal with dimensions 10mm x 10mm x 6mm. Model No. HO-LDP-10, wavelength range 200-2200nm, was placed to remove any polarization component present in the scattered light. (Hanzlíková et al., 1999)

To monitor pressure for both enantiomers, fine ruby powder was used. The R1 and R2 distinct ruby peaks were observed under a non-hydrostatic pressure. R1 ruby fluorescence line was used for calibration purposes. (Mao et al., 1986) Within the gasket cavity, chunks of fine ruby powder were placed at three locations. Pressure was measured by averaging the pressure readings from three locations. We monitored the R1 ruby fluorescence line to calibrate pressure. The Raman optical activity setup on which the experiment was performed is shown in Figure 6.3.

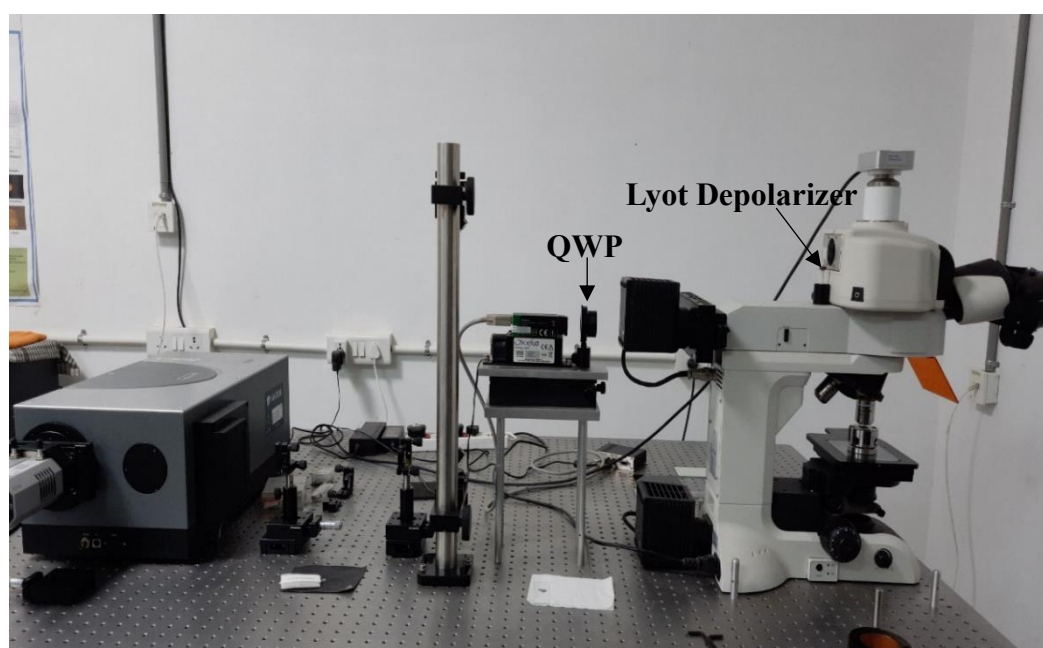


Figure 6.3: Modified Raman setup to record Raman optical activity (ROA) of chiral samples. QWP stands for quarter wave plate.

6.3 Results and Discussions

Ambient Raman Spectra of R BINAP and S BINAP recorded in the range from 63-3171 cm^{-1} is shown in Figure 6.5. The spectrum exhibits significant modes owing to vibrational modes correlated to 1,1'- Bi-2-naphthol (BINOL). BINOL is an organic chiral compound also used in asymmetric synthesis and also exist in two enantiomeric forms. It possesses axial chirality and forerunner to BINAP. The structure of BINOL is shown in Figure 6.4 with atom designations. BINAP mode assignments are done in accordance with BINOL due to the similarity in chemical structure and the presence of axial chirality in both. (Li et al., 2007)

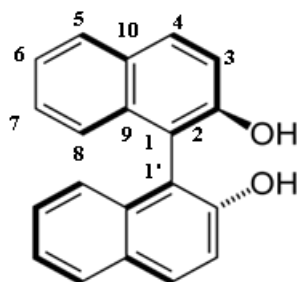


Figure 6.4: Schematic of structural diagram of BINOL with numbering of atoms.

Raman modes at the ambient condition of solid 1,1'- Bi-2-naphthol (BINOL) shows prominent modes at ν , bond stretching ($\sim 1031 \text{ cm}^{-1}$, 1271 cm^{-1} , 1378 cm^{-1} , 1438 cm^{-1} , 1591 cm^{-1} , 1622 cm^{-1}), τ , out-of-plane (naphthyl) torsion of carbon atoms ($\sim 418 \text{ cm}^{-1}$, 439 cm^{-1} , 489 cm^{-1}), τ_{butt} , ($\sim 245 \text{ cm}^{-1}$), butterfly torsion between two naphthyl rings, γ , out-of-plane (naphthyl) wagging of hydrogen atoms ($\sim 418 \text{ cm}^{-1}$, 439 cm^{-1} , 489 cm^{-1} , 793 cm^{-1}), δ , in-plane (naphthyl) bond bending ($\sim 524 \text{ cm}^{-1}$, 850 cm^{-1} , 956 cm^{-1} , 1031 cm^{-1} , 1271 cm^{-1} , 1378 cm^{-1} , 1591 cm^{-1} , 1622 cm^{-1}). In addition to these modes, several weak modes exist. Normalized ambient Raman spectra of R BINAP and S BINAP are shown in Figure 6.5. R BINAP is shown with a **black line**, while S BINAP is shown with a **red line**. The spectra of both enantiomers completely overlap each other.

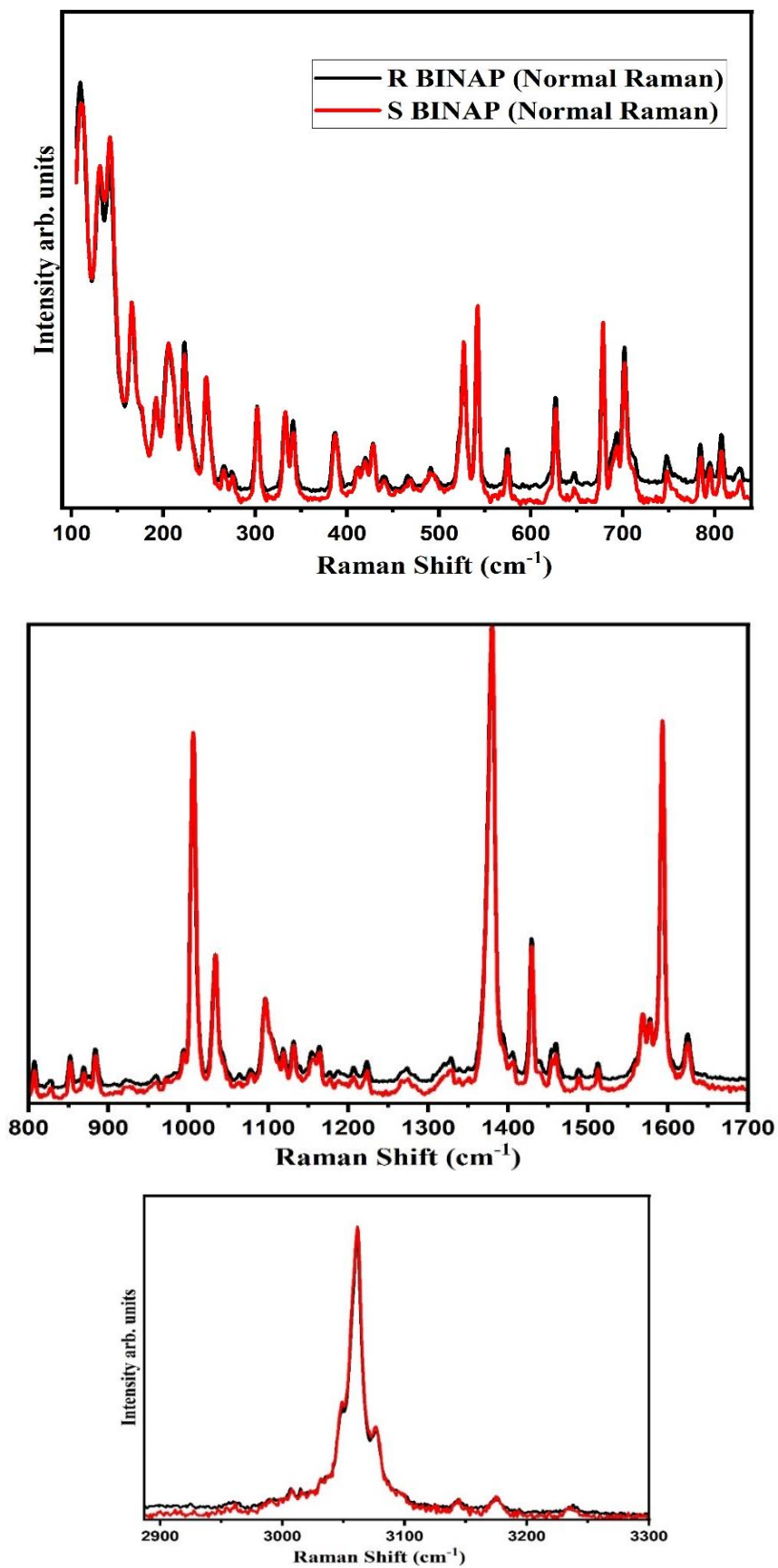


Figure 6.5: Normalized ambient Raman spectra of R BINAP (black line) and S BINAP (red line).

Mode assignments and representation of modes

BINAP mode assignments are shown in Table 6.1 and are done in accordance with BINOL due to the similarity in chemical structure and the presence of axial chirality in both molecules.

Table 6.1: Raman modes at ambient condition of solid 1,1'-Bi-2-naphthol (BINOL) excited at 514.5 nm. ν , bond stretching; τ , out-of-plane (naphthyl) torsion of carbon atoms; τ_{butt} , butterfly torsion between two naphthyl rings; γ , out-of-plane (naphthyl) wagging of hydrogen atoms, δ , in-plane (naphthyl) bond bending.

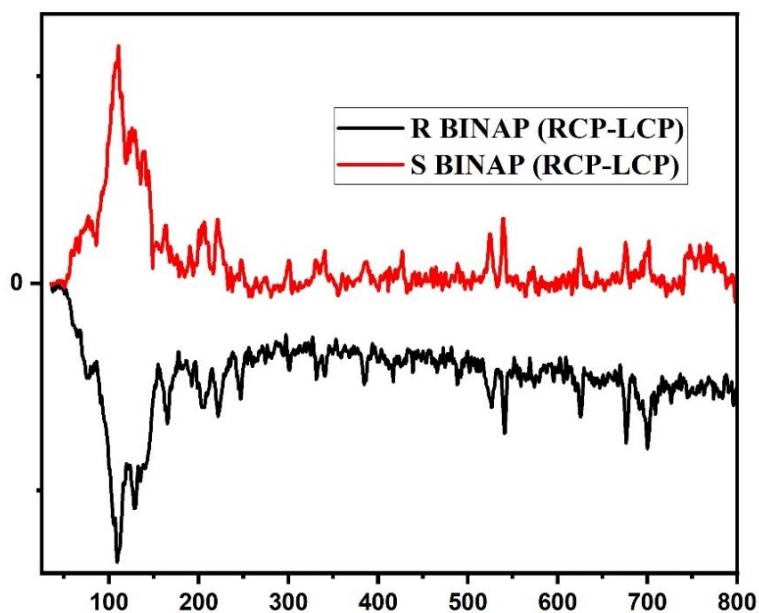
(Li et al., 2007) (Nogueira & Quintal, 2000)

Raman Frequency (cm ⁻¹)	Assignments
245	τ_{butt}
418	τ_{C_5} , τ_{C_8} , τ_{C_3} , $\gamma_{\text{C}_5\text{-H}}$, $\gamma_{\text{C}_8\text{-H}}$, $\gamma_{\text{C}_3\text{-H}}$
426	τ_{CC}
439	τ_{C_9} , $\tau_{\text{C}_{10}}$, τ_{C_5} , τ_{C_8} , $\gamma_{\text{C}_5\text{-H}}$, $\gamma_{\text{C}_8\text{-H}}$
489	τ_{C_9} , $\tau_{\text{C}_{10}}$, τ_{C_5} , τ_{C_8} , $\gamma_{\text{C}_5\text{-H}}$, $\gamma_{\text{C}_8\text{-H}}$, $\gamma_{\text{C}_4\text{-H}}$
524	$\delta_{\text{C}_6\text{-C}_7\text{-C}_8}$, $\delta_{\text{C}_9\text{-C}_{10}\text{-C}_5}$, $\delta_{\text{C}_2\text{-C}_3\text{-C}_4}$
539	$\delta_{\text{C-C}}$
793	$\gamma_{\text{C}_8\text{-H}}$, $\gamma_{\text{C}_3\text{-H}}$, $\gamma_{\text{C}_4\text{-H}}$, $\gamma_{\text{C}_5\text{-H}}$
850	$\delta_{\text{C}_3\text{-C}_4\text{-C}_{10}}$, $\delta_{\text{C}_6\text{-C}_7\text{-C}_8}$
956	$\delta_{\text{C}_1\text{-C}_2\text{-C}_3}$, $\delta_{\text{C}_{10}\text{-C}_5\text{-C}_6}$, $\delta_{\text{C}_6\text{-C}_7\text{-C}_8}$, $\delta_{\text{C}_8\text{-C}_9\text{-C}_{10}}$
1031	$\nu_{\text{C}_6\text{-C}_7}$, $\delta_{\text{C}_6\text{-C}_7\text{-C}_8}$, $\delta_{\text{C}_5\text{-C}_6\text{-C}_7}$, $\delta_{\text{C}_5\text{-H}}$, $\delta_{\text{C}_6\text{-H}}$, $\delta_{\text{C}_7\text{-H}}$, $\delta_{\text{C}_8\text{-H}}$,
1152	$\delta_{\text{C-H}}$,
1271	$\nu_{\text{C-O}}$, $\nu_{\text{C}_8\text{-C}_9}$, $\delta_{\text{C}_5\text{-H}}$, $\delta_{\text{C}_7\text{-H}}$, $\delta_{\text{C}_8\text{-H}}$
1378	$\nu_{\text{C}_9\text{-C}_{10}}$, $\delta_{\text{O-H}}$, $\nu_{\text{C}_2\text{-O}_{11}}$
1403	–
1438	$\nu_{\text{C}_7\text{-C}_8}$, $\nu_{\text{C}_1\text{-C}_9}$, $\nu_{\text{C}_{10}\text{-C}_5}$

1591	$\nu_{C_1-C_1'}, \nu_{C_2-C_3}, \nu_{C_6-C_7}, \nu_{C_9-C_{10}}, \delta_{O-H}$
1622	$\nu_{C_1-C_2}, \nu_{C_2-O_{11}}, \nu_{C_3-O_4}, \nu_{C_5-C_6}, \nu_{C_7-C_8}, \delta_{O-H}$
3059	ν_{CH}

Incident Circular Polarization Raman Optical Activity (ICP ROA) Spectra of R BINAP and S BINAP

The vibrational incident circularly polarized Raman optical activity (ICP ROA) spectra of R BINAP (**black**) and S BINAP (**red**) are shown in Figure 6.6. Both of the spectra are recorded in backscattering geometry in the range of 63-3171 cm^{-1} . The ROA spectra of R BINAP and S BINAP were compared and observed to be mirror images of each other. The S BINAP ROA spectrum is positive, while the R BINAP spectrum was found to be negative. The spectra of both samples were recorded in the DAC at ambient conditions, and the diamond peak is observed at 1338 cm^{-1} . In both spectra, diamond peaks overlap each other as it is an achiral molecule and does not show ROA.



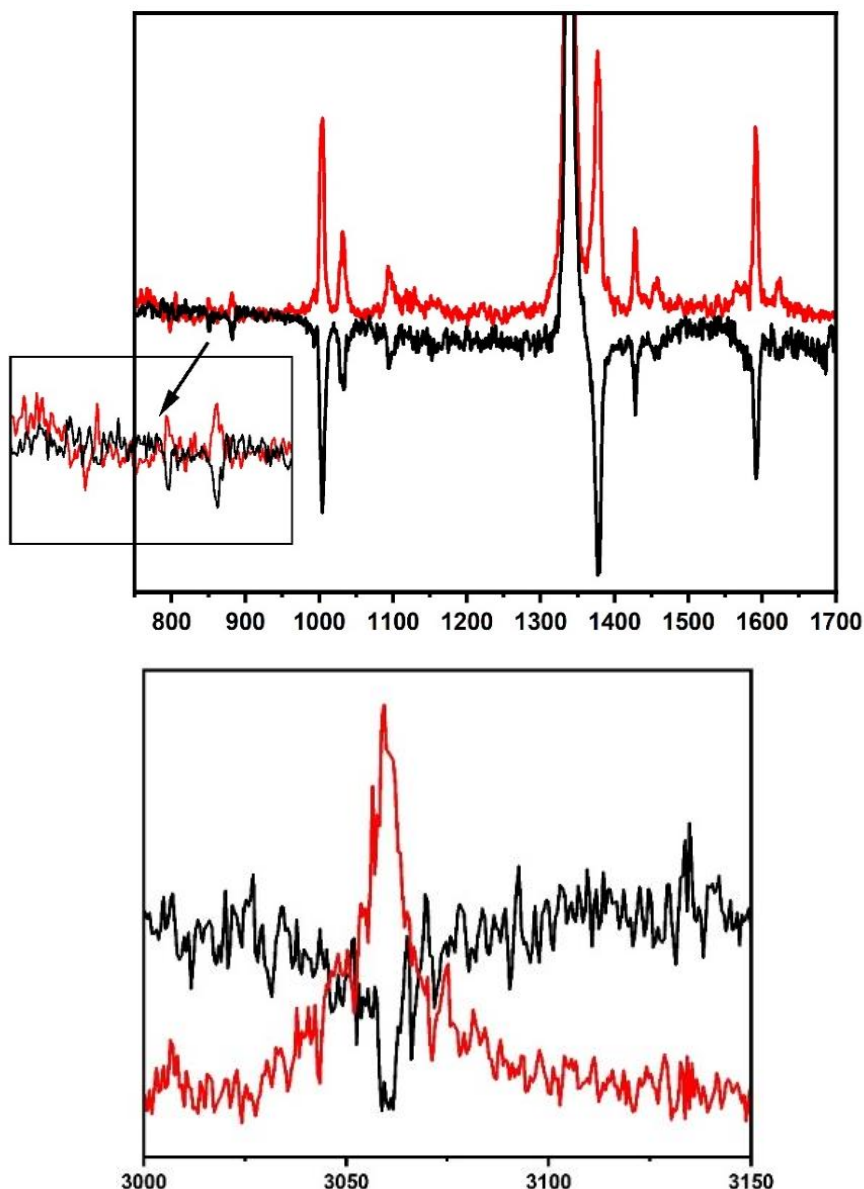


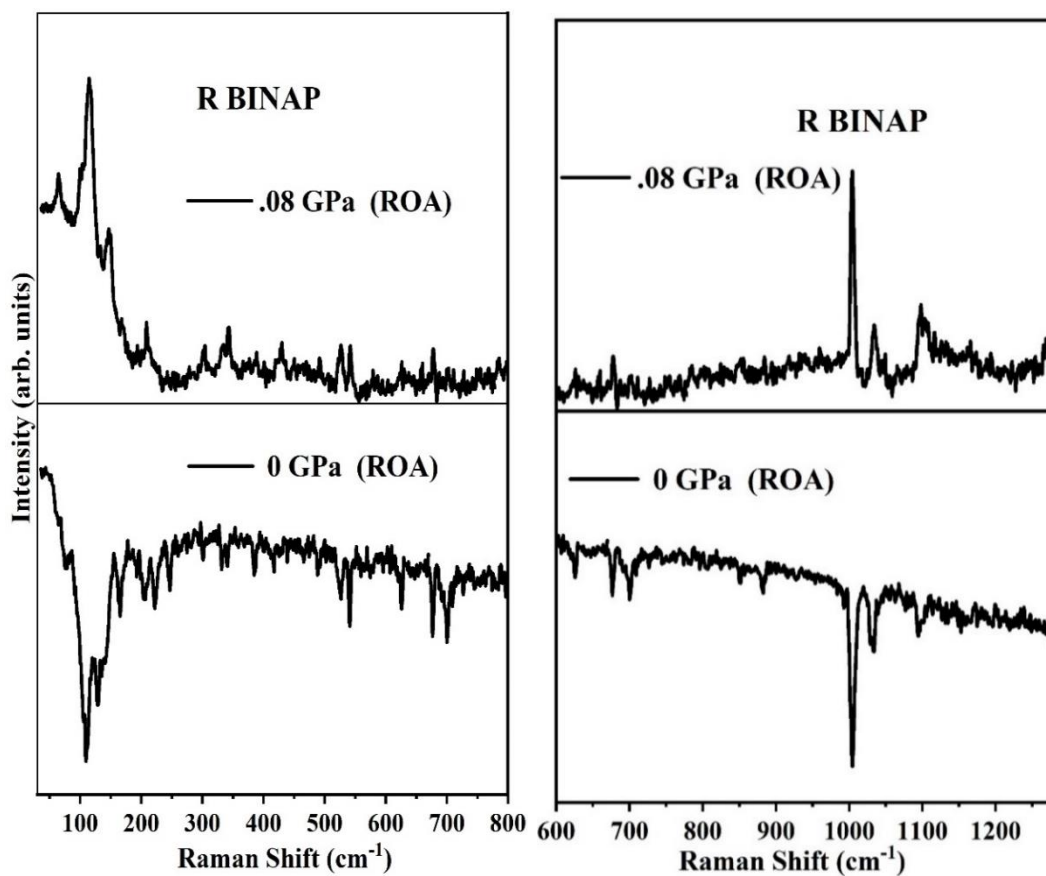
Figure 6.6: Ambient Raman Optical Activity (ROA) spectra of R BINAP (black line) and S BINAP (red line).

High pressure Raman Optical Activity study of R BINAP and S BINAP (2, 2'- bis (diphenyl phosphino)- 1,1' binaphthyl) in non-hydrostatic pressure environment

The high-pressure ROA spectra of R BINAP subjected to non-hydrostatic pressure conditions are shown in Figure 6.7. R BINAP peaks were observed negative at 0 GPa but were switched to positive peaks at a low pressure of 0.08 GPa. With an increase in non-hydrostatic pressure of 0.08 GPa, the chirality of R BINAP was found to be switched as all modes present in R BINAP at ambient conditions were found to be switched at 0.08 GPa.

Above 0.08 GPa, the sample (R BINAP) was further compressed at 0.36 GPa, and no chirality was observed except for 1378 cm^{-1} ($\nu_{\text{C}_9\text{-C}_{10}}$, $\delta_{\text{O-H}}$, $\nu_{\text{C}_2\text{-O}_{11}}$), as shown in Figure 6.8 . On

further compression, no ROA was observed. The experiment was performed up to 11.77 GPa and only normal Raman spectra could be recorded due to lack of any ROA. With decompression, ROA spectra was not reversible and no switching back of chirality was observed in R BINAP.



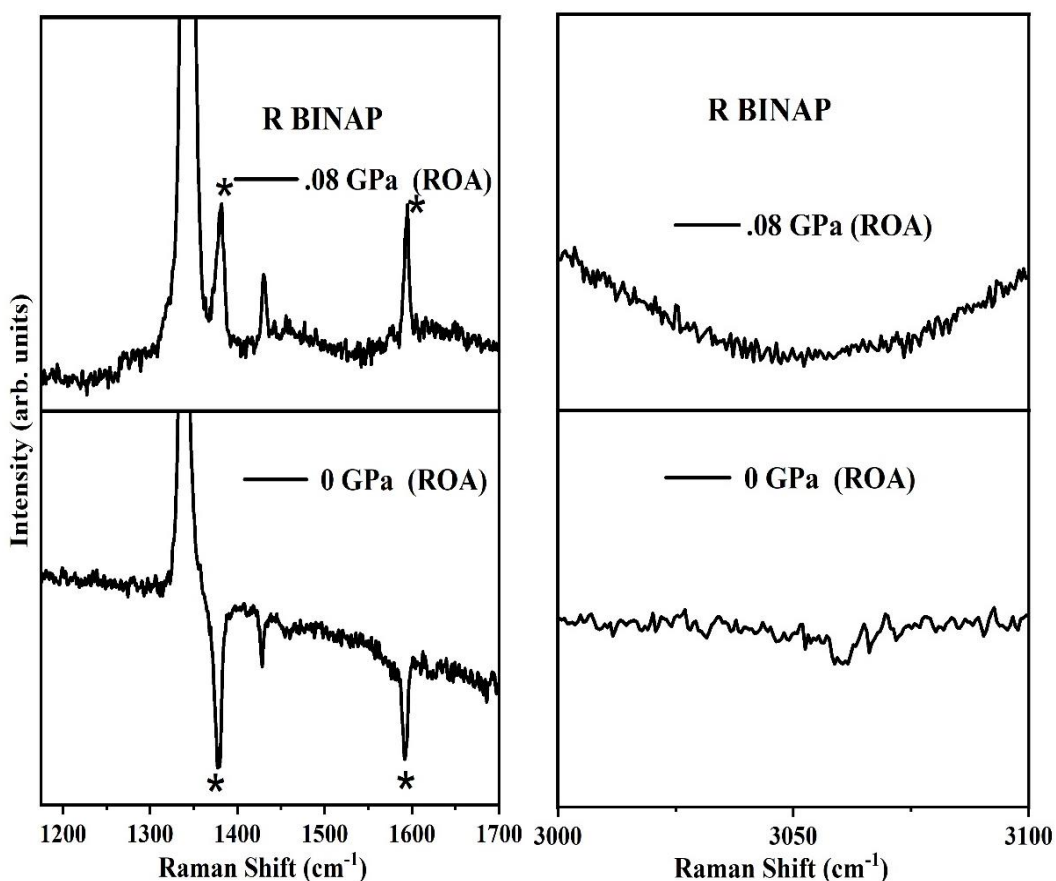


Figure 6.7: Raman Optical activity (ROA) spectra of **R BINAP** at 0 GPa and 0.08 GPa.

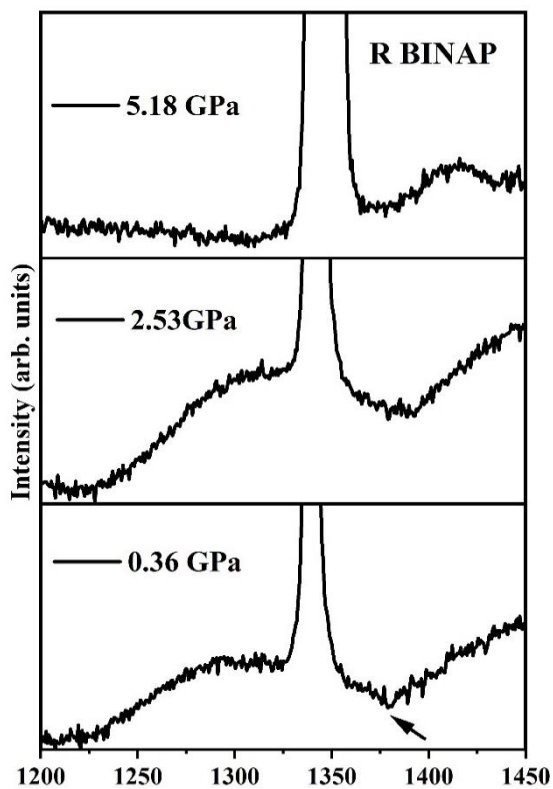


Figure 6.8: Raman Optical activity (ROA) observed stretching mode $\sim 1378 \text{ cm}^{-1}$ **R BINAP** with compression.

The high-pressure ROA spectra of S BINAP subjected to non-hydrostatic pressure conditions are shown in Figure 6.9. ROA spectra of S BINAP were found to be positive, and once 0.08 GPa pressure was applied to the sample, the maximum number of peaks present in spectra switched to negative. Peaks that were not switched at 0.08 GPa were $\sim 1378\text{ cm}^{-1}$ ($\nu\text{C}_9\text{-C}_{10}$, $\delta\text{O-H}$, $\nu\text{C}_2\text{-O}_{11}$) and $\sim 1427\text{ cm}^{-1}$. On further increase in pressure, at 0.14 GPa, $\sim 1378\text{ cm}^{-1}$ peak ($\nu\text{C}_9\text{-C}_{10}$, $\delta\text{O-H}$, $\nu\text{C}_2\text{-O}_{11}$) switched from positive to negative while $\sim 1427\text{ cm}^{-1}$ mode just vanished. With decompression, only $\sim 1378\text{ cm}^{-1}$ ($\nu\text{C}_9\text{-C}_{10}$, $\delta\text{O-H}$, $\nu\text{C}_2\text{-O}_{11}$) peak was reversed, but it was extremely weak in intensity, and no other peak showed reversibility.

Results indicate that a small pressure of 0.08 GPa is able to switch the chirality of S BINAP as can be observed from Figure 6.9. The switched chirality for $\sim 1378\text{ cm}^{-1}$ ($\nu\text{C}_9\text{-C}_{10}$, $\delta\text{O-H}$, $\nu\text{C}_2\text{-O}_{11}$) was observed for few more pressures (around 2 GPa) as shown in Figure 6.10. On further compression, no ROA was observed in the sample, no chirality and no switching back of chirality was observed. Non reversibility of ROA spectra indicate structural change and change in characteristic properties of chiral molecule.

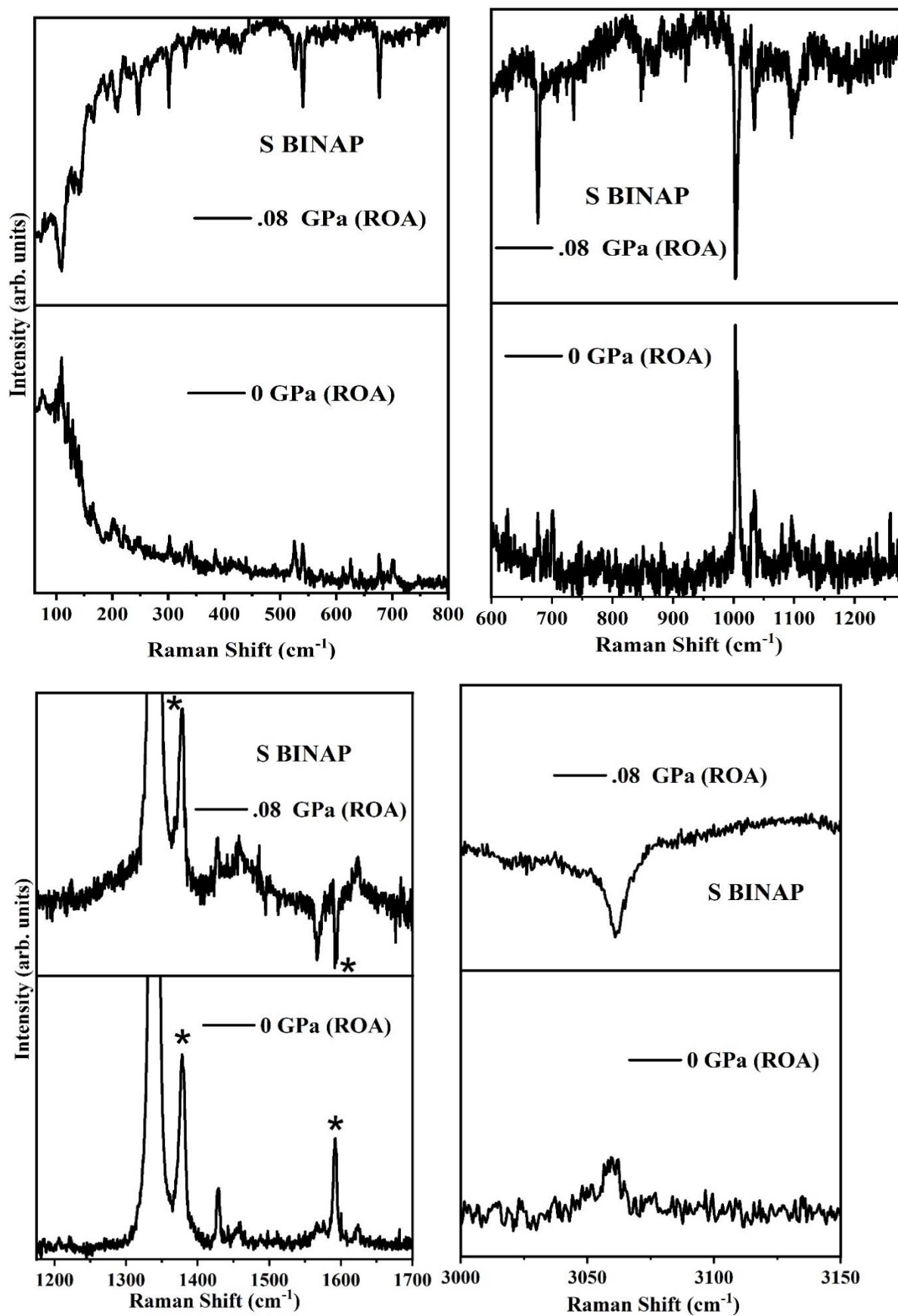


Figure 6.9: Raman Optical activity (ROA) spectra of S BINAP at 0 GPa and 0.08 GPa.

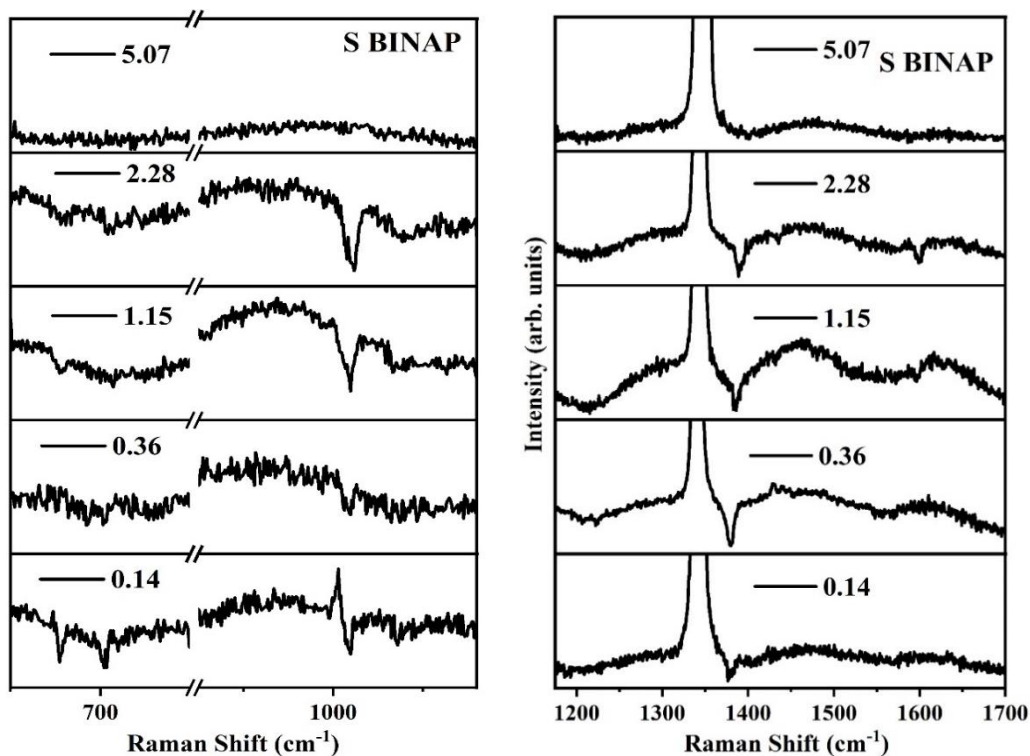


Figure 6.10: Raman Optical activity (ROA) spectra of **S BINAP** with compression.

High pressure Raman study of **R BINAP** (2, 2'- bis (diphenyl phosphino)- 1,1' binaphthyl) in non-hydrostatic pressure environment

High pressure Raman spectra of $C_{44}H_{32}P_2$ (**R BINAP**) (2, 2'- bis (diphenyl phosphino)- 1,1' binaphthyl) subjected to non-hydrostatic pressure conditions from 0 to 11.77 GPa is shown in Figure 6.11. The Raman spectra of **R BINAP** show that a number of weak peaks disappear at very low pressure of 0.08 GPa, $\sim 1031\text{ cm}^{-1}$ (νC_6-C_7 , $\delta C_6-C_7-C_8$, $\delta C_5-C_6-C_7$, δC_5-H , δC_6-H , δC_7-H , δC_8-H) splits at low frequency. Pressure induced changes were observed again at 0.36 GPa where $\sim 418\text{ cm}^{-1}$ (τC_5 , τC_8 , τC_3 , γC_5-H , γC_8-H , γC_3-H), and $\sim 426\text{ cm}^{-1}$ (τCC) were observed to be merged. $\sim 524\text{ cm}^{-1}$ ($\delta C_6-C_7-C_8$, $\delta C_9-C_{10}-C_5$, $\delta C_2-C_3-C_4$) splits at low frequency side and begins to merge with 539 cm^{-1} ($\delta C-C$) at 0.36 GPa. At same pressure, mode $\sim 700\text{ cm}^{-1}$ develops a split at high frequency side. These changes in Raman spectra clearly signify at 0.36 GPa, **R BINAP** undergoes some structural changes.

Major pressure induced changes were observed at 2.53 GPa. At this pressure, $\sim 539\text{ cm}^{-1}$ ($\delta C-C$) and $\sim 676\text{ cm}^{-1}$ modes dropped in intensity. $\sim 1031\text{ cm}^{-1}$ (νC_6-C_7 , $\delta C_6-C_7-C_8$, $\delta C_5-C_6-C_7$, δC_5-H , δC_6-H , δC_7-H , δC_8-H) splits and develops a new shoulder peak at high frequency. The

mode $\sim 1378\text{ cm}^{-1}$ ($\nu_{\text{C}_9\text{-C}_{10}}$, $\delta_{\text{O-H}}$, $\nu_{\text{C}_2\text{-O}_{11}}$) develops a shoulder peak at high frequency side. Modes $\sim 1566\text{ cm}^{-1}$ and $\sim 1576\text{ cm}^{-1}$ present on the left of hinge mode 1591 cm^{-1} ($\nu_{\text{C}_1\text{-C}_1'}$, $\nu_{\text{C}_2\text{-C}_3}$, $\nu_{\text{C}_6\text{-C}_7}$, $\nu_{\text{C}_9\text{-C}_{10}}$, $\delta_{\text{O-H}}$), both started merging together. $\sim 1622\text{ cm}^{-1}$ ($\nu_{\text{C}_1\text{-C}_2}$, $\nu_{\text{C}_2\text{-O}_{11}}$, $\nu_{\text{C}_3\text{-O}_4}$, $\nu_{\text{C}_5\text{-C}_6}$, $\nu_{\text{C}_7\text{-C}_8}$, $\delta_{\text{O-H}}$) mode is observed till maximum pressure of 2.53 GPa.

$\sim 1031\text{ cm}^{-1}$ and $\sim 1378\text{ cm}^{-1}$ modes begin to split at 2.53 GPa, and the splitting increases significantly, and hinge mode was merged with other peaks present on low frequency side. On compression, all modes were found to be shifted. These striking changes indicate the phase transition at 2.53 GPa. Raman measurements indicate major changes in molecular structure and the possible formation of achiral molecule under high pressure. Changes due to the induced pressure in non-hydrostatic environment on R BINAP are summarized in Figure 6.13.

Decompression data is shown in Figure 6.12, on decompression, modes $\sim 1378\text{ cm}^{-1}$ ($\nu_{\text{C}_9\text{-C}_{10}}$, $\delta_{\text{O-H}}$, $\nu_{\text{C}_2\text{-O}_{11}}$) and 1591 cm^{-1} ($\nu_{\text{C}_1\text{-C}_1'}$, $\nu_{\text{C}_2\text{-C}_3}$, $\nu_{\text{C}_6\text{-C}_7}$, $\nu_{\text{C}_9\text{-C}_{10}}$, $\delta_{\text{O-H}}$) were partially reversible with respect to peak positions but peak intensities are not recovered and other modes present in ambient spectra were not reversible. The non-reversibility of Raman spectra indicates a change in molecular structure.

A systematic study of the vibrational spectra (Raman) of chiral molecules indicates that a small pressure of 0.08 GPa splits peak $\sim 1031\text{ cm}^{-1}$ ($\nu_{\text{C}_6\text{-C}_7}$, $\delta_{\text{C}_6\text{-C}_7\text{-C}_8}$, $\delta_{\text{C}_5\text{-C}_6\text{-C}_7}$, $\delta_{\text{C}_5\text{-H}}$, $\delta_{\text{C}_6\text{-H}}$, $\delta_{\text{C}_7\text{-H}}$, $\delta_{\text{C}_8\text{-H}}$) in low frequency side and affects weak peaks. Splitting of $\sim 1031\text{ cm}^{-1}$ ($\nu_{\text{C}_6\text{-C}_7}$, $\delta_{\text{C}_6\text{-C}_7\text{-C}_8}$, $\delta_{\text{C}_5\text{-C}_6\text{-C}_7}$, $\delta_{\text{C}_5\text{-H}}$, $\delta_{\text{C}_6\text{-H}}$, $\delta_{\text{C}_7\text{-H}}$, $\delta_{\text{C}_8\text{-H}}$), and $\sim 1378\text{ cm}^{-1}$ ($\nu_{\text{C}_9\text{-C}_{10}}$, $\delta_{\text{O-H}}$, $\nu_{\text{C}_2\text{-O}_{11}}$) indicates high pressure interaction between neighbouring molecules. In the low pressure region, pressure induced changes were observed at 0.36 GPa indicating some structural disturbance in the molecule.

Further, at 2.53 GPa major pressure induced changes were observed. Peaks $\sim 1031\text{ cm}^{-1}$ ($\nu_{\text{C}_6\text{-C}_7}$, $\delta_{\text{C}_6\text{-C}_7\text{-C}_8}$, $\delta_{\text{C}_5\text{-C}_6\text{-C}_7}$, $\delta_{\text{C}_5\text{-H}}$, $\delta_{\text{C}_6\text{-H}}$, $\delta_{\text{C}_7\text{-H}}$, $\delta_{\text{C}_8\text{-H}}$) and $\sim 1378\text{ cm}^{-1}$ ($\nu_{\text{C}_9\text{-C}_{10}}$, $\delta_{\text{O-H}}$, $\nu_{\text{C}_2\text{-O}_{11}}$) split at this pressure, and new peaks appeared at 2.53 GPa, it strongly suggest formation of new bonds and a change in the chemical structure of chiral molecule. Further, with pressure, no other splitting were observed, but a reduction in peak intensities was observed. $\sim 1622\text{ cm}^{-1}$ ($\nu_{\text{C}_1\text{-C}_2}$, $\nu_{\text{C}_2\text{-O}_{11}}$, $\nu_{\text{C}_3\text{-O}_4}$, $\nu_{\text{C}_5\text{-C}_6}$, $\nu_{\text{C}_7\text{-C}_8}$, $\delta_{\text{O-H}}$) mode was not observed above 2.53 GPa, signifying structural change. Modes $\sim 1566\text{ cm}^{-1}$ and $\sim 1576\text{ cm}^{-1}$ present on the left of hinge mode 1591 cm^{-1} ($\nu_{\text{C}_1\text{-C}_1'}$, $\nu_{\text{C}_2\text{-C}_3}$, $\nu_{\text{C}_6\text{-C}_7}$, $\nu_{\text{C}_9\text{-C}_{10}}$, $\delta_{\text{O-H}}$) both start merging with it indicating pressure induced change in the structure of molecule.

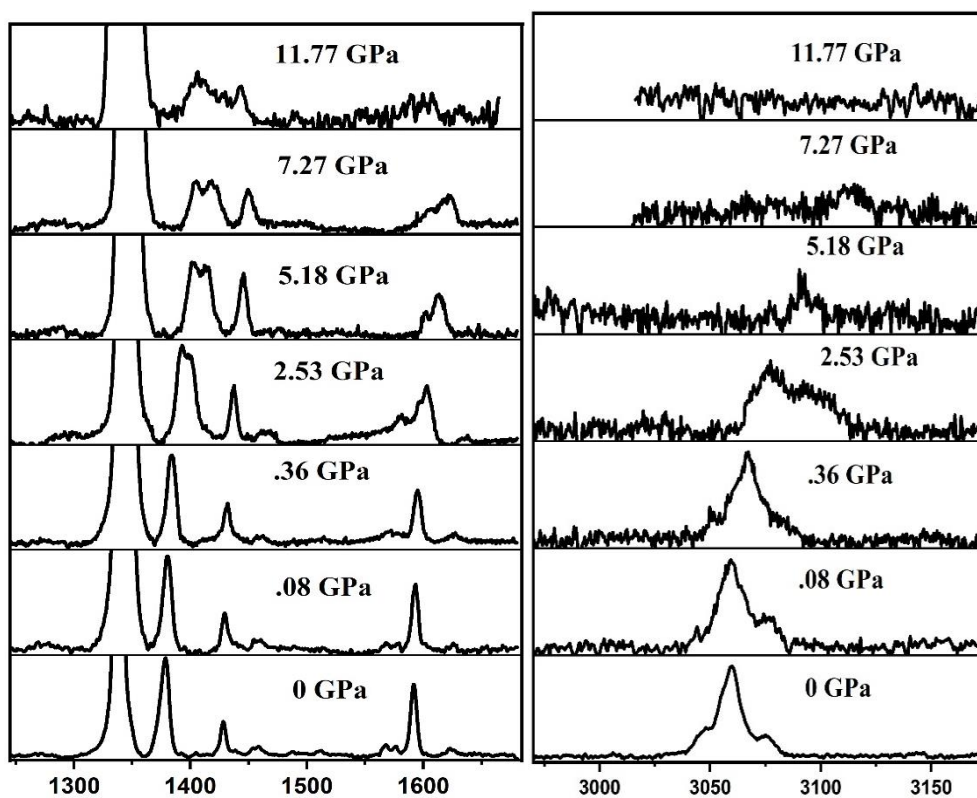
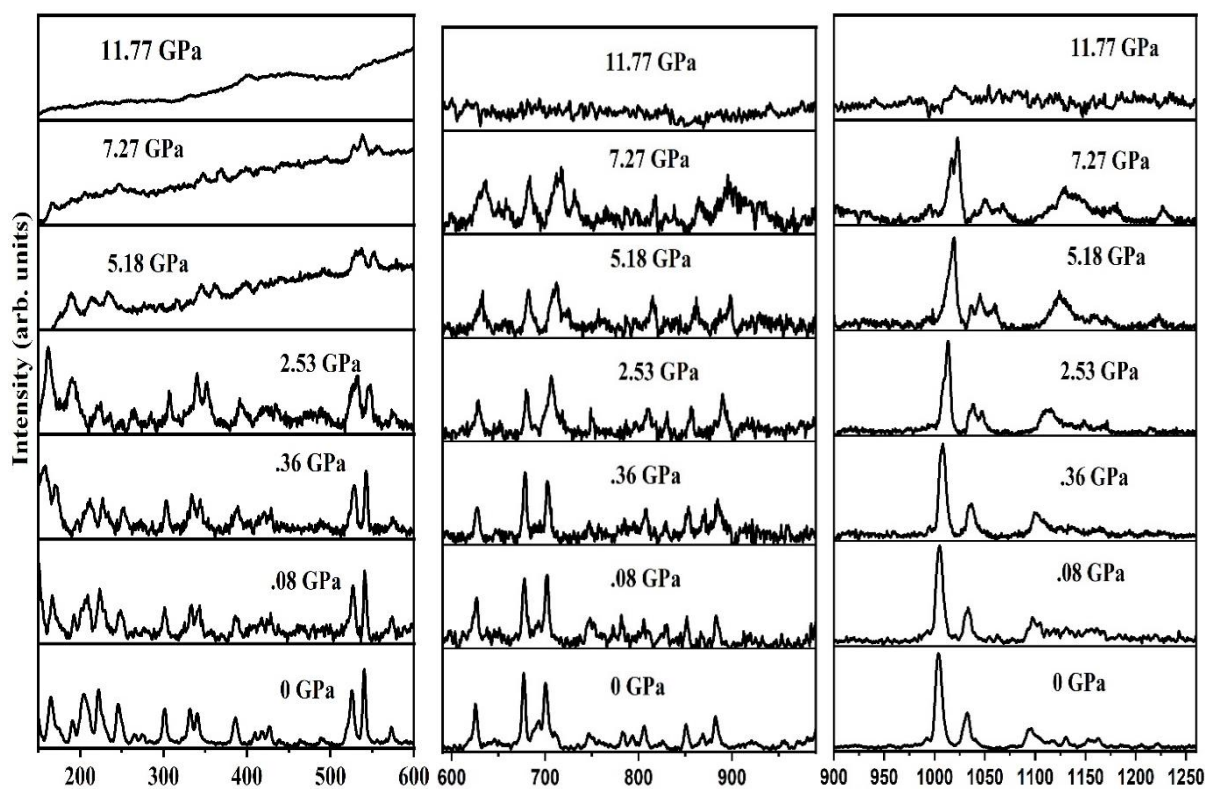


Figure 6.11: Raman spectra of **R BINAP** (2, 2'- bis (diphenyl phosphino)- 1,1' binaphthyl) at non-hydrostatic pressure (0-11.77GPa).

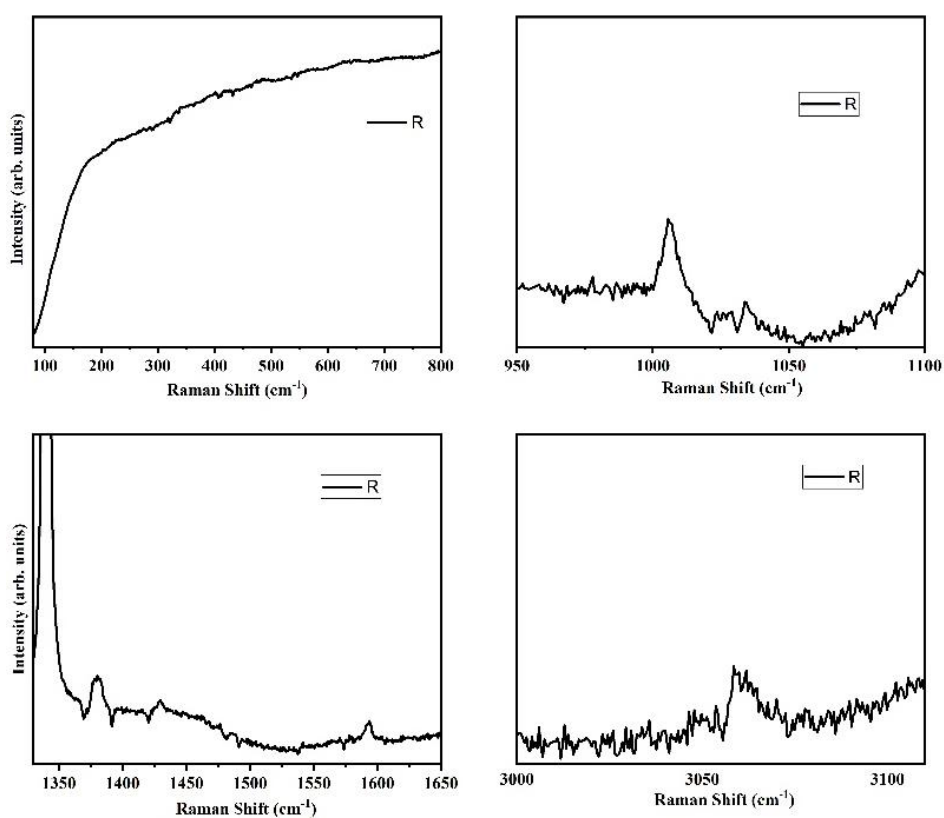
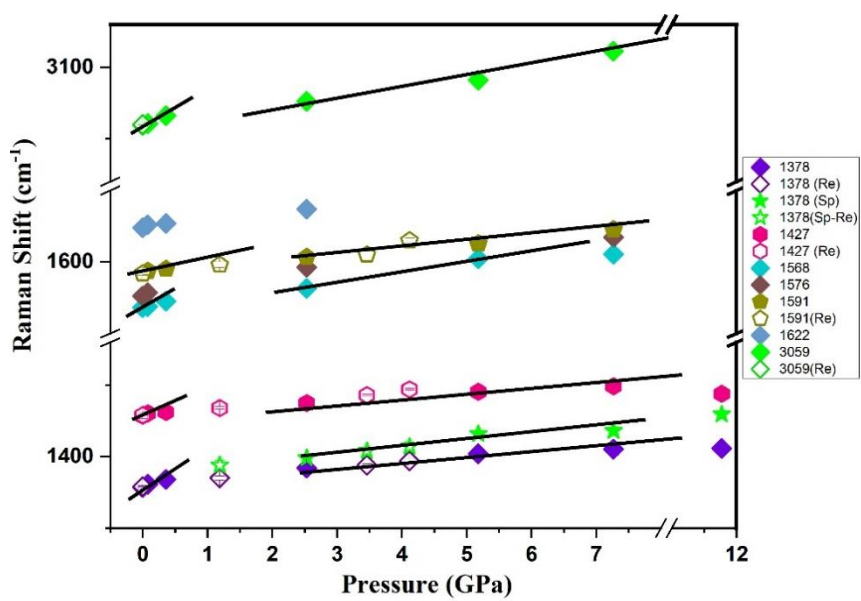


Figure 6.12: Raman spectra of solid R BINAP. (fully decompressed)



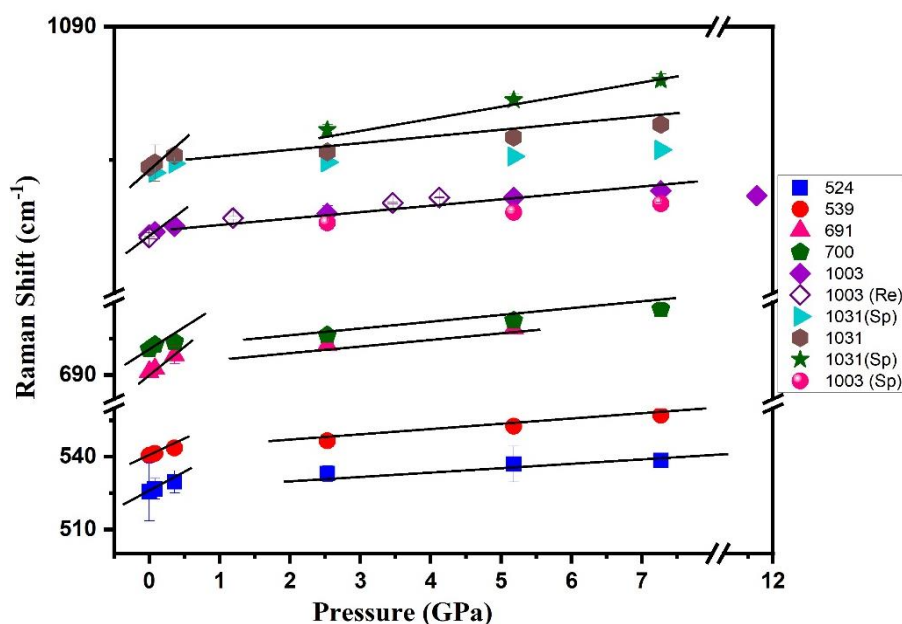
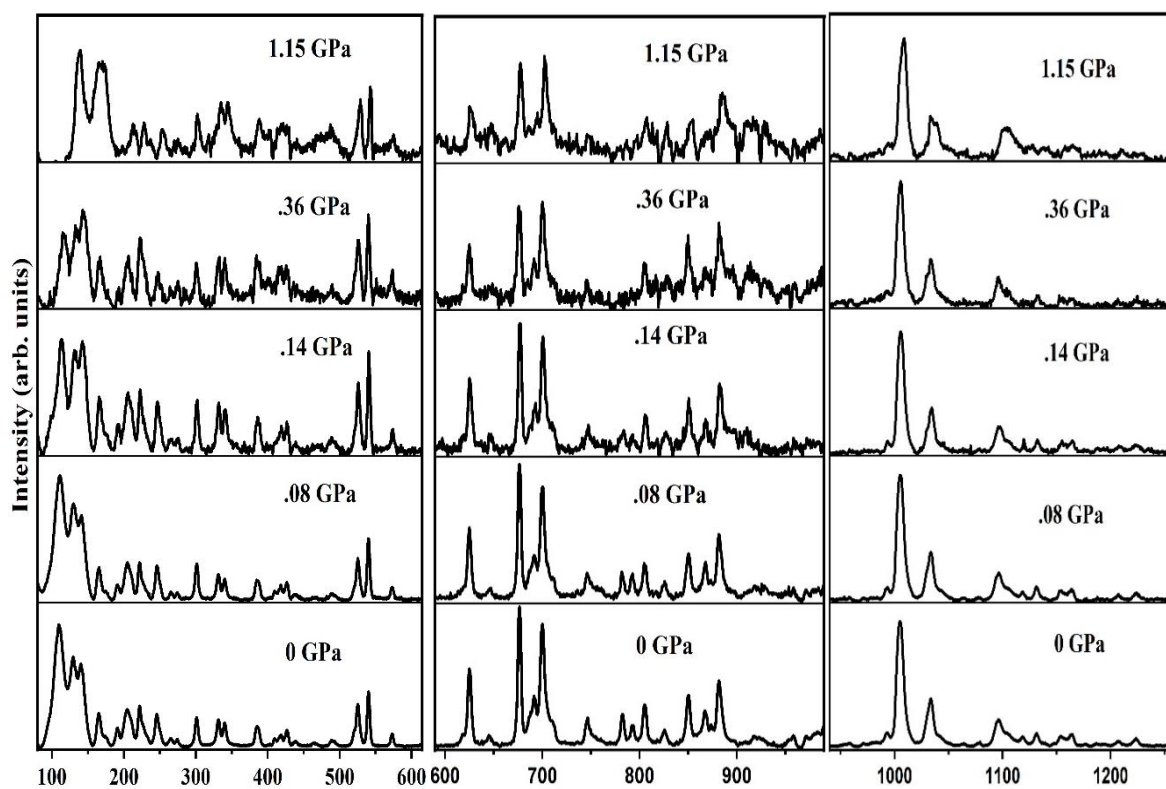
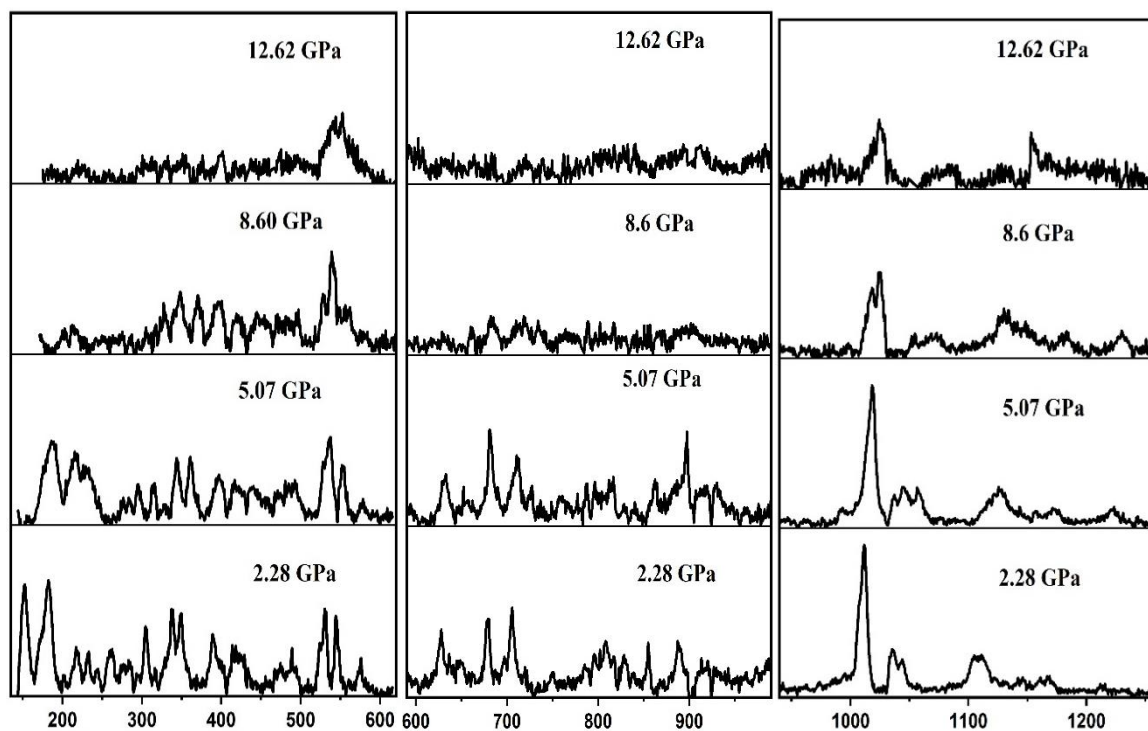


Figure 6.13: Pressure dependence of Raman modes under non-hydrostatic pressure. The filled symbols denote compression and open symbols denote decompression. In ω vs P plot, Sp and Re labels are used to indicate splitted peaks, and reversible peaks.

High pressure study of S BINAP (2, 2'- bis (diphenyl phosphino)- 1,1' binaphthyl) in non-hydrostatic pressure environment

High pressure Raman spectra of $C_{44}H_{32}P_2$ (S BINAP) (2, 2'- bis (diphenyl phosphino)- 1,1' binaphthyl) subjected to non-hydrostatic pressure conditions from 0 to 12.62 GPa are shown in Figure 6.14. The Raman spectra of S BINAP show similar behavioural changes as R BINAP, as shown in Figure 6.11. At 0.36 GPa pressure induced changes were observed.

Major pressure induced changes were observed at 2.28 GPa. At this pressure, Splitting and merging of peaks and phase change of S BINAP is similar to R BINAP. These noticeable changes suggests a phase transition at around 2 GPa. On decompression, the Raman spectra were not completely reversible. Modes $\sim 1378\text{ cm}^{-1}$ (νC_9-C_{10} , $\delta O-H$, νC_2-O_{11}) and 1591 cm^{-1} ($\nu C_1-C_1'$, νC_2-C_3 , νC_6-C_7 , νC_9-C_{10} , $\delta O-H$) were reversible but only with respect to the peak positions but not with respect to the peak intensities, as can be observed from Figure 6.15. Pressure dependence of Raman modes under non-hydrostatic pressure is shown in Figure 6.16. Decompression data reveals that the molecule makes an effort to recover from structural change but was unable to do that. *in-situ* high pressure Raman spectroscopic studies of both enantiomers of 2,2' bis (diphenylphosphino)-1,1'-binaphthyl) ($C_{44}H_{32}P_2$) show similar changes.



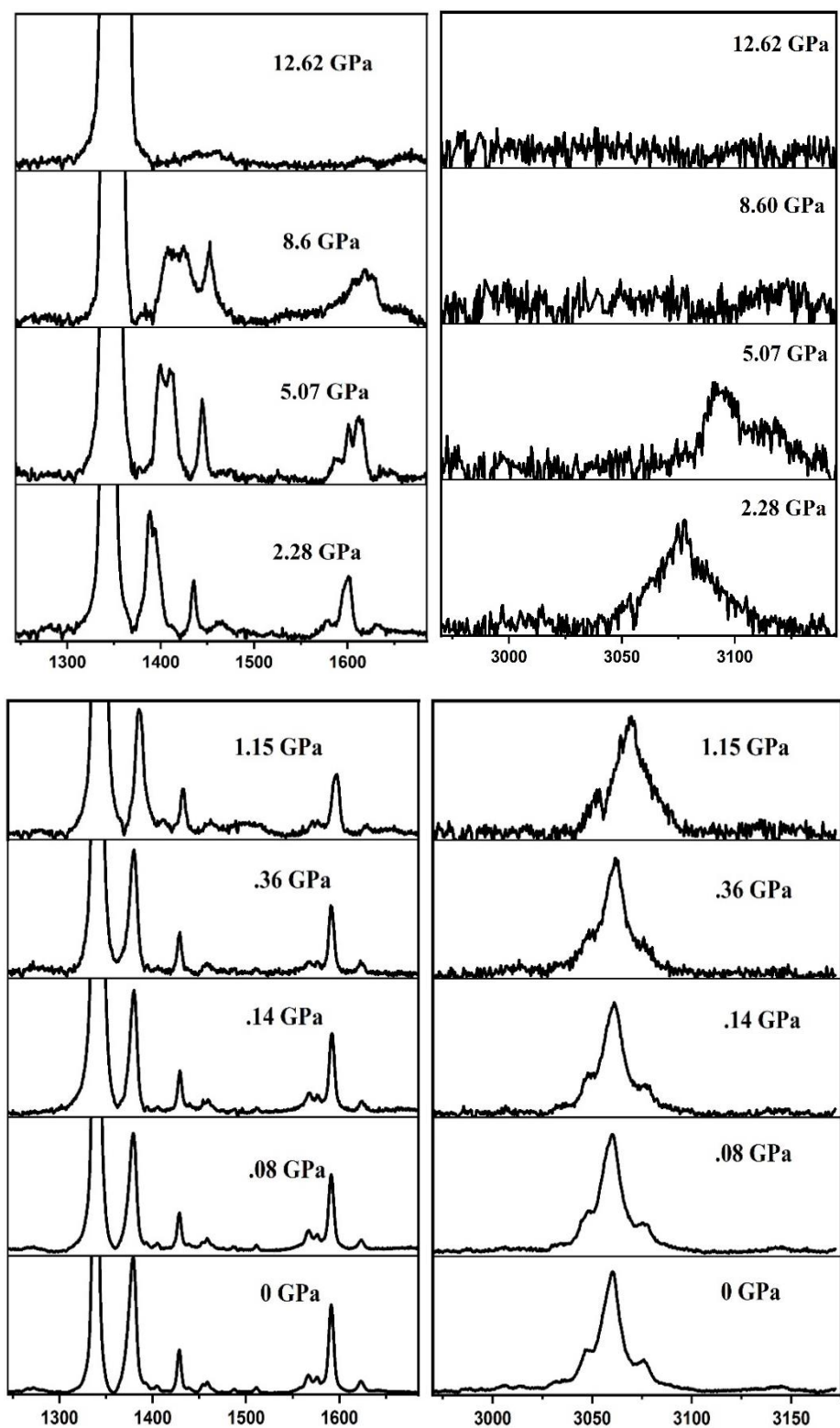


Figure 6.14: Raman spectra of **S BINAP** (2, 2'- bis (diphenyl phosphino)- 1,1' binaphthyl) at non-hydrostatic pressure (0-12.62GPa).

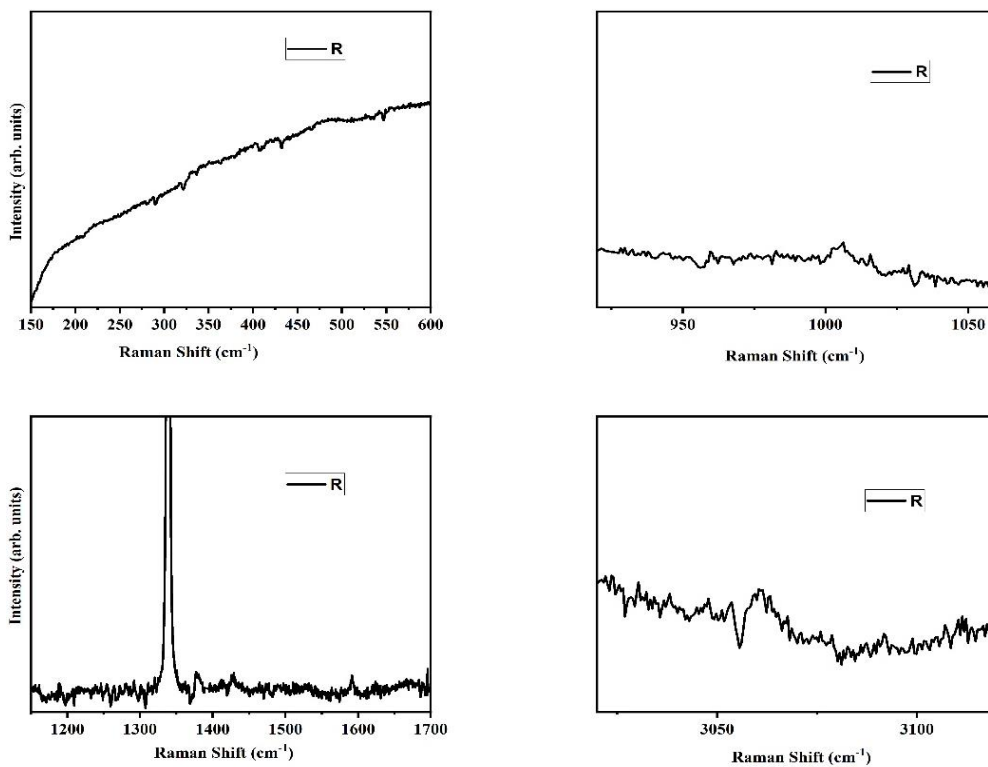
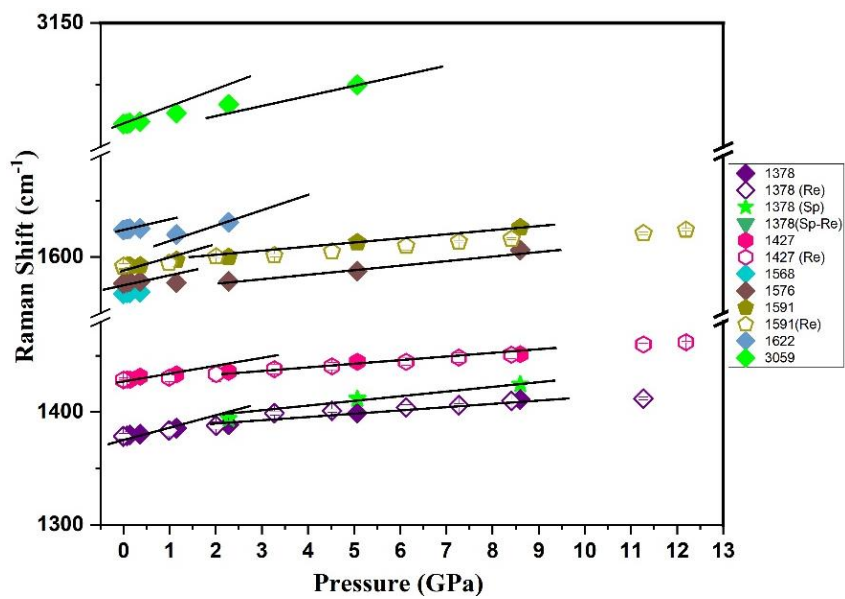


Figure 6.15: Decompression stack plot of **S BINAP**.



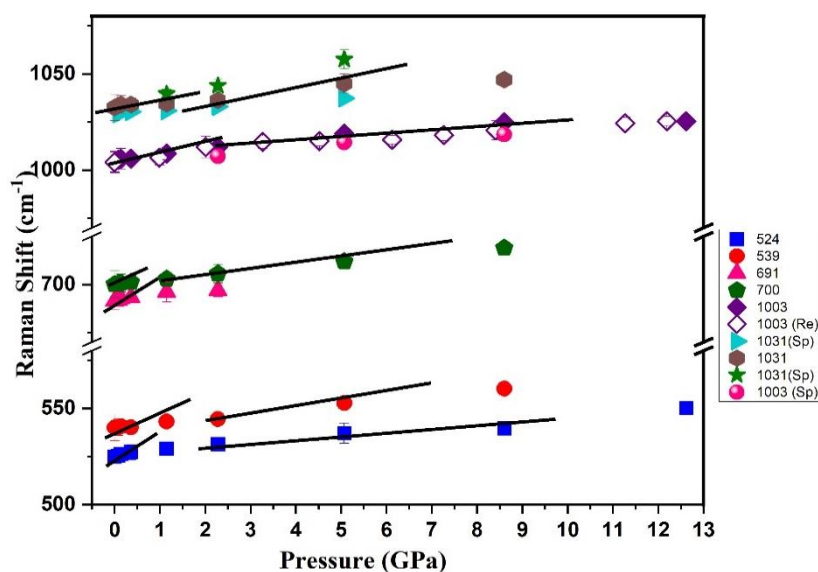


Figure 6.16: Pressure dependence of Raman modes under non-hydrostatic pressure for **S BINAP**. The filled symbols denote compression and open symbols denote decompression. Sp and Re labels are used to indicate splitted and reversible peaks.

In summary, to check changes in the optical handedness of enantiomeric molecules with pressure, *in-situ* high pressure Raman optical activity (ROA) and high pressure Raman measurements on chiral molecules were carried out. No such studies are available in the literature, and to the best of our knowledge, ours is the first high pressure ROA study being reported on chiral materials. It is very important to know the change in effectiveness of the chiral medicine after the pelletization process as during the pelletization process, external pressure is applied.

It has been observed that the ROA spectra of both enantiomers were exactly mirror images of each other at ambient conditions. A small pressure of 0.08 GPa switches the chirality of both enantiomers. After 0.08 GPa, chirality was observed for mode $\sim 1378 \text{ cm}^{-1}$ ($\nu_{\text{C}_9\text{-C}_{10}}$, $\delta_{\text{O-H}}$, $\nu_{\text{C}_2\text{-O}_{11}}$) and it was observed up to a maximum pressure of 2 GPa. Beyond 2.53 GPa for R BINAP and 2.28 GPa for S BINAP, no chirality in the molecule was observed. A maximum pressure of 11.77 GPa was applied on R BINAP and 12.62 GPa on S BINAP and no switching back of chirality was observed. With decompression, ROA spectra was not reversible for R BINAP but for S BINAP few peaks were reversible with respect to peak position with some hysteresis with respect to peak intensity. Thus, due to compression, the structure of the molecule has changed which can surely affect the chiral properties of molecules.

These results are associated with major structural changes in both chiral enantiomers, and it is possible that under small external stress (0.08 GPa), both samples are switching their chirality. On decompression from 11.77GPa for R BINAP and 12.22 GPa for S BINAP, the Raman spectrum is not completely reversible; it reveals a pressure induced change in the three dimensional stereoisomeric structure of the chiral molecules.

Most of the drugs in the pharmaceutical industry are made up of chiral compounds, therefore its essential to know their chirality. These results will be of significant benefit to the pharmaceutical industry, as enantiomers can change their chirality during pelletization, which may change the functionality of the drug molecule, making it possibly hazardous.

6.4 Conclusion

In our work, we elucidate a systematic high-pressure Raman optical activity study on both enantiomers of $C_{44}H_{32}P_2$ in a non-hydrostatic pressure environment. At ambient pressure, both enantiomers show the opposite ROA, but at low pressure of 0.08 GPa, both enantiomers switch their chirality. On further compression, no switching back of chirality is observed. With decompression, no reversibility in the ROA spectra is observed. Normal Raman spectra of both enantiomers show phase change at 0.36 GPa and major pressure induced changes at 2.53 GPa. Raman spectra show merging of modes $\sim 1566\text{ cm}^{-1}$ and $\sim 1576\text{ cm}^{-1}$ to hinge mode (1591 cm^{-1}). Our study indicate both enantiomers of chiral molecule (BINAP) show phase change and structural change at same pressures.¹ With decompression, the normal Raman spectra are not completely reversible for both enantiomers. Some of the peaks are reversible but very weak in terms of intensity. Our experimental results are new and are of very fundamental importance to the pharmaceutical industry, as both enantiomers are switching their chirality at very low pressures comparable to those used in tableting.